Phase Diagram of QCD

M.A. STEPHANOV
Physics Department, University of Illinois, 845 W. Taylor St., Chicago, IL 60607-7059, USA

This is a brief summary of the contemporary understanding of the QCD phase diagram as a function of temperature T and baryo-chemical potential μ_B.

1 Introduction

Strong interactions are described by Quantum Chromodynamics (QCD) – a remarkable theory. QCD is a convincing practical example of the success of the quantum field theory. Asymptotic freedom allows QCD to be consistent down to arbitrary short distance scale, enabling us to define the theory completely in terms of the fundamental microscopic degrees of freedom – quarks and gluons. This fundamental definition is very simple, yet the theory describes a wide range of phenomena – from the mass spectrum of hadrons to deep-inelastic processes. As such, QCD should also possess well defined thermodynamic properties. The knowledge of QCD thermodynamics is essential for the understanding of such natural phenomena as compact stars and laboratory experiments involving relativistic heavy-ion collisions.

Full analytical treatment of QCD is very difficult. In certain limits, in particular, for large values of the external thermodynamic parameters temperature T and/or baryo-chemical potential μ_B, when thermodynamics is dominated by short-distance QCD dynamics, the theory can be studied analytically, due to the asymptotic freedom. But the most interesting experimental region of parameters T and μ_B is that of order $\Lambda_{\rm QCD}$ – the intrinsic QCD scale. This makes first principle lattice approaches, which do not rely on a small coupling expansion, an invaluable and the most powerful tool in studying QCD thermodynamics.

The full potential of lattice methods is close to being realized as far as the study of QCD at $\mu_B = 0$ is concerned. The status of thermodynamics of QCD at *non-zero* μ_B is different. The main impediment to lattice simulations is the notorious sign problem. No method devised so far is known, or expected, to converge to the correct physical result as the infinite volume limit is approached at *fixed* $\mu_B \neq 0$. However, since the most interesting structure of the QCD phase diagram (phase transitions and critical points) lie at nonzero μ_B, any progress in this direction is especially valuable. Existing lattice methods generically rely on clever extrapolations from $\mu_B = 0$. These techniques yield interesting results in the regime of small, but already experimentally relevant μ_B.

A contemporary view of the QCD phase diagram is shown in Fig. 1. It is a compilation of a body of results from model calculations, empirical nuclear physics, as well as first principle lattice QCD calculations and perturbative calculations in asymptotic regimes.

This report provides an overview of the structure of the QCD phase diagram based on available theoretical (lattice and model calculations) and phenomenological input.

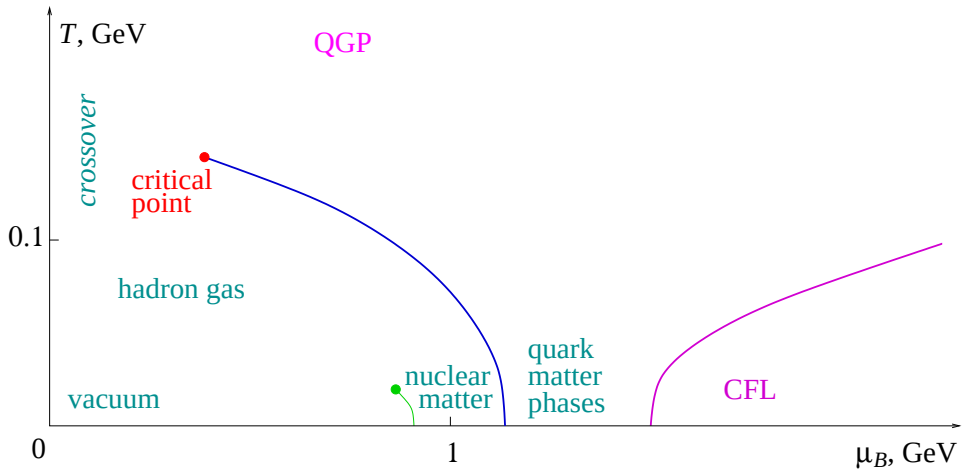

Figure 1: The contemporary view of the QCD phase diagram – a semiquantitative sketch.

2 The phase diagram

Thermodynamic properties of a system are most readily expressed in terms of a phase diagram in the space of thermodynamic parameters – in the case of QCD – as a $T\mu_B$ phase diagram. Each point on the diagram corresponds to a stable thermodynamic state, characterized by various thermodynamic functions, such as, e.g., pressure, baryon density, etc. (as well as kinetic coefficients, e.g., diffusion or viscosity coefficients, or other properties of various correlation functions).

Static thermodynamic quantities can be derived from the partition function – a Gibbs sum over eigenstates of QCD Hamiltonian, which can be alternatively expressed as a path integral in Euclidean space of the exponent of the QCD action.

2.1 Massless quark limit and chiral symmetry argument

In the chiral limit – the idealized limit when 2 lightest quarks, u and d, are taken to be massless, the Lagrangian of QCD acquires chiral symmetry $\mathrm{SU}(2)_L \times \mathrm{SU}(2)_R$, corresponding to SU(2) flavor rotations of (u_L, d_L) and (u_R, d_R) doublets independently. The ground state of QCD breaks the chiral symmetry spontaneously locking $\mathrm{SU}(2)_L$ and $\mathrm{SU}(2)_R$ rotations into a single vector-like $\mathrm{SU}(2)_V$ (isospin) symmetry and generating 3 massless Goldstone pseudoscalar bosons – the pions. The breaking of the chiral symmetry is a non-perturbative phenomenon.

At sufficiently high temperature $T \gg \Lambda_{\mathrm{QCD}}$, due to the asymptotic freedom of QCD, perturbation theory around the approximation of the gas of free quarks and gluons (quark-gluon plasma – QGP) should become applicable. In this regime chiral symmetry is not broken. Thus we must expect a transition from a broken chiral symmetry vacuum state to a chirally symmetric equilibrium state at some temperature $T_c \sim \Lambda_{\mathrm{QCD}}$. The transition is akin to the Curie point in a ferromagnet – where the rotational O(3) symmetry is restored by thermal fluctuations (chiral $\mathrm{O}(4)=\mathrm{SU}(2)\times\mathrm{SU}(2)$ symmetry in QCD). Thermodynamic functions of QCD must be singular at the transition point – as always when the transition separates thermodynamic states of different global symmetry.

Thus, in the massless quark (chiral) limit, the region of broken chiral symmetry on the $T\mu_B$ phase diagram must be separated from the region of the restored symmetry by a closed boundary.

2.2 $N_{\rm f} = 2$ *chiral limit and tricritical point*

For *two massless* quarks the transition can be either second or first order [1]. As lattice and model calculations show, both possibilities are realized depending on the value of the strange quark mass m_s and/or the baryo-chemical potential μ_B.

The point on the chiral phase transition line where the transition changes order is called tricritical point. The location of this point is one of the unknowns of the QCD phase diagram with 2 massless quarks. In fact, even the order of the transition at $\mu_B = 0$, which many older and recent studies suggest is of the second order is still being questioned (see review [2]).

Neither can it be claimed reliably (model or assumption independently) that the transition, if it begins as a 2nd order at $\mu_B = 0$, changes to first order at larger μ_B. However, numerous model calculations show this is the case. Lattice calculations also support such a picture. Contemporary understanding of QCD at low T and large μ_B, recently reviewed in [3], also point at a first order transition (at low-T, high-μ_B) from nuclear matter to color-superconducting quark matter phase.

2.3 *Physical quark masses and crossover*

When the up and down quark masses are set to their observed finite values, the diagram assumes the shape sketched in Fig. 1. The second order transition line (where there was one) is replaced by a crossover – the criticality needed for the second order chiral restoration transition requires tuning chiral symmetry breaking parameters (quark masses) to zero. In the absence of the exact chiral symmetry (broken by quark masses) the transition from low- to high-temperature phases of QCD need not proceed through a singularity. Lattice simulations do indeed show that the transition is a crossover for $\mu_B = 0$ (most recently and decisively Ref.[4], see also Ref.[2] for a review).[a] Recent terminology for the QCD state near the crossover ($T \sim (1-2)T_c$) is *strongly coupled quark-gluon plasma* (sQGP).

Transport properties of sQGP have attracted considerable attention. For example, generally, the shear viscosity η is a decreasing function of the coupling strength. The dimensionless ratio of $\eta/\hbar$ to the entropy density s tends to infinity asymptotically far on either side of the crossover – in dilute hadron gas ($T \to 0$) and in asymptotically free QGP ($T \to \infty$). Near the crossover η/s should thus be expected to reach a minimum [5]. The viscosity can be indirectly determined in heavy ion collisions by comparing hydrodynamic calculations to experimental data. Such comparison [6] indeed indicates that the viscosity (per entropy density) of this "crossover liquid" is relatively small, and plausibly is saturating the lower bound conjectured in Ref. [7].

2.4 *Physical quark masses and the critical point*

The first order transition line is now ending at a point known as the QCD critical point or end point.[b] The end point of a first order line is a critical point of the second order. This is by far the most common critical phenomenon in condensed matter physics. Most liquids possess such a singularity, including water. The line which we know as the water boiling transition ends at pressure $p = 218$ atm and $T = 374°$C in a critical point.

Beside the critical point, the phase diagram of QCD in Fig. 1 has other similarities with the phase diagram of water. A number of ordered quark matter phases must exist in the low-T high-μ_B region, which are akin to many (more than 10) confirmed phases of ice. For asymptotically large μ_B, QCD with 3 quark flavors must be in color-flavor locked (CFL) state [8,3].

[a] This fact is technically easier to establish than the order of the transition in the chiral limit – taking the chiral limit is an added difficulty.

[b] The QCD critical point is sometimes also referred to as *chiral* critical point which sets it apart from another known (nuclear) critical point, the end-point of the transition separating nuclear liquid and gas phases (see Fig. 1). This point occurs at much lower temperatures $\mathcal{O}(10MeV)$ set by the scale of the nuclear binding energies.

3 Locating the critical point: the sign problem

The critical point is a well-defined singularity on the phase diagram, and it appears as an attractive theoretical, as well as experimental, target to shoot at. Theoretically, finding the coordinates (T, μ_B) of the critical point is a straightforwardly defined task. We need to calculate the partition function of QCD and find the singularity corresponding to the end of the first order transition line. But it is easier said than done.

Of course, calculating such a path integral analytically is beyond present reach. Numerical lattice Monte Carlo simulations is an obvious tool to choose for this task. At zero μ_B Monte Carlo method allows us to determine the equation of state of QCD as a function of T (and show that the transition is a crossover). However, at *finite* μ_B the Nature guards its secrets better.

The notorious sign problem has been known to lattice Monte Carlo experts since the early days of this field. Calculating the partition function using Monte Carlo method hinges on the fact that the exponent of the Euclidean action S_E is a positive-definite function of its variables (values of the fields on the lattice). This allows one to limit calculation to a relatively small set of field configurations randomly picked with probability proportional to the value of $\exp(-S_E)$.

In QCD with $\mu_B \neq 0$ the Monte Carlo action $S_{\rm MC}$ (playing the role of S_E) is complex. With $S_{\rm MC}$ complex, how does one pick configurations? A number of ways to circumvent the problem have been tried. For example, using the modulus of $\exp(-S_{\rm MC})$ as a probability measure, or the value of $\exp(-S_{\rm MC})$ at *zero* μ_B, when it is still positive. Unfortunately, none of the methods can be expected to converge to correct result with the increasing lattice volume V, unless this limit is accompanied by an exponential $\exp(\mathrm{const}\cdot V)$ increase of the number of configurations, rendering Monte Carlo technique useless.

In the absence of a reliable first-principle approach model calculations have been the main source of knowledge about the QCD phase diagram [9,10,11,12,13,14,15,16,17,18]. This situation has began to change recently.

4 Lattice approaches to finding the critical point

This section is devoted to brief (and necessarily incomplete) descriptions of currently developed lattice methods for reaching out into the $T\mu_B$ plane. For a more comprehensive description of these methods, as well as other methods not discussed here, the reader may consult the most up-to-date reviews [19,20] as well as an earlier review by Philipsen [21], which also contain further references to original papers.

4.1 Reweighting

The first lattice prediction for the location of the critical point was reported by Fodor and Katz in Ref. [22]. The assumption is that, although the problem becomes exponentially difficult as $V \to \infty$, in practice, one can get a sensible approximation at finite V. In addition, simulations at finite T might suffer lesser overlap problem because of large thermal fluctuations [23]. One can hope that if the critical point is at a small value of μ_B, the volume V may not need to be too large to achieve a reasonable accuracy.

4.2 Imaginary μ_B and $N_{\rm f} = 3$

By the universality argument of Ref. [1], the finite temperature transition is 1st order for $m_u = m_d = m_s = 0$. By continuity, it must remain 1st order in a finite domain of the $m_s m_{ud}$ plane (taking $m_u = m_d \equiv m_{ud}$) surrounding the origin – the plot of this domain is known as Columbia plot [24,2]. For physical quark masses and $\mu_B = 0$ the temperature driven transition is a crossover,

which means that the physical point is outside of the 1st order domain in the $m_s m_{ud}$ plot. Reducing quark masses should pull the point into the 1st order domain.

What happens to the critical point when (m_s, m_{ud}) is in the 1st order domain? It is still a singularity of the partition function as a function of μ_B, but it moves out into the complex μ_B plane. More precisely, it moves onto *imaginary* μ_B axis. This remarkable fact allows one to look at (the complex descendant of) the critical point in a direct Monte Carlo simulation – since there is no sign problem for imaginary μ_B. This observation is at the core of the method developed by de Forcrand and Philipsen [25,26].

4.3 Taylor expansion

Taylor expansion in μ_B is another method to circumvent the sign problem. Derivatives of pressure (or other thermodynamic quantities) are calculated at $\mu_B = 0$ and assembled into a Taylor series expansion to obtain dependence of that quantity on μ_B [27,28,29]

At fixed temperature, the convergence radius of the Taylor expansion in μ_B is limited by the nearest singularity in the complex plane of μ_B. Assuming that at the temperature T_E, at which the critical point (T_E, μ_E) occurs on the phase diagram, this critical point is the nearest singularity to $\mu_B = 0$, one could use Taylor expansion to determine μ_E [27,28,29,19], if T_E is known.

Assuming that the radius of convergence μ_R can be approximated using the first few terms of the Taylor expansion, the main remaining problem is to determine the value of T_E i.e., to identify at which value of T the complex singularity reaches the real axis in the μ_B plane. This question has been addressed using universality arguments, as well as an example random matrix calculation in Ref[30].

5 Scanning QCD phase diagram in heavy ion collisions

Even though the exact location of the critical point is not known to us yet, the available theoretical estimates suggest that the point is within the region of the phase diagram probed by the heavy-ion collision experiments. This raises the possibility to discover this point in such experiments [31].

It is known empirically that with increasing collision energy, $\sqrt{s}$, the resulting fireballs tend to freeze out at decreasing values of μ_B, i.e., decreasing baryon-antibaryon asymmetry. This is easy to understand, since the amount of generated entropy (heat) grows with $\sqrt{s}$ while the net baryon number is limited by that number in the initial nuclei.

The information about the location of the freezeout point for given experimental conditions is obtained by measuring the ratios of particle yields (e.g., baryons or antibaryons to pions), and fitting to a statistical model with T and μ_B as parameters [32].

As with any critical point, measurement of fluctuations can be used to determine when the system is in the vicinity of the critical point. By measuring variables sensitive to the proximity of the critical point as a function of monotonically increasing $\sqrt{s}$ of the collision, and observing non-monotonic dependence, one discovers the critical point [31]. The values of $T\mu_B$ corresponding to the freezeout at such a value of $\sqrt{s}$ give the coordinates of the critical point.

Acknowledgments

This work is supported by the DOE (DE-FG0201ER41195).

References

1. R. D. Pisarski and F. Wilczek, Phys. Rev. D **29** (1984) 338.

2. U. Heller, PoS(LAT2006)011.
3. M. Alford, PoS(LAT2006)001.
4. K. Szabo, PoS(LAT2006)149.
5. L. P. Csernai, J. I. Kapusta and L. D. McLerran, Phys. Rev. Lett. **97**, 152303 (2006) [arXiv:nucl-th/0604032].
6. D. Teaney, Phys. Rev. C **68**, 034913 (2003) [arXiv:nucl-th/0301099].
7. P. Kovtun, D. T. Son and A. O. Starinets, Phys. Rev. Lett. **94**, 111601 (2005) [arXiv:hep-th/0405231].
8. M. G. Alford, K. Rajagopal and F. Wilczek, Nucl. Phys. B **537** (1999) 443 [arXiv:hep-ph/9804403].
9. M. Asakawa and K. Yazaki, Nucl. Phys. A **504** (1989) 668.
10. A. Barducci, R. Casalbuoni, S. De Curtis, R. Gatto and G. Pettini, Phys. Lett. B **231** (1989) 463; Phys. Rev. D **41** (1990) 1610.
11. A. Barducci, R. Casalbuoni, G. Pettini and R. Gatto, Phys. Rev. D **49** (1994) 426.
12. J. Berges and K. Rajagopal, Nucl. Phys. B **538** (1999) 215 [arXiv:hep-ph/9804233].
13. M. A. Halasz, A. D. Jackson, R. E. Shrock, M. A. Stephanov and J. J. M. Verbaarschot, Phys. Rev. D **58** (1998) 096007 [arXiv:hep-ph/9804290].
14. O. Scavenius, A. Mocsy, I. N. Mishustin and D. H. Rischke, Phys. Rev. C **64** (2001), 045202 [arXiv:nucl-th/0007030].
15. N. G. Antoniou and A. S. Kapoyannis, Phys. Lett. B **563** (2003) 165 [arXiv:hep-ph/0211392].
16. Y. Hatta and T. Ikeda, Phys. Rev. D **67** (2003) 014028 [arXiv:hep-ph/0210284].
17. A. Barducci, R. Casalbuoni, G. Pettini and L. Ravagli, Phys. Rev. D **72**, 056002 (2005) [arXiv:hep-ph/0508117].
18. S. Roessner, C. Ratti and W. Weise, arXiv:hep-ph/0609281.
19. C. Schmidt, PoS(LAT2006)021.
20. M. A. Stephanov, PoS(LAT2006)024 [arXiv:hep-lat/0701002].
21. O. Philipsen, PoS(LAT2005)016 [arXiv:hep-lat/0510077].
22. Z. Fodor and S. D. Katz, JHEP **0203** (2002) 014 [arXiv:hep-lat/0106002]; JHEP **0404**, 050 (2004) [arXiv:hep-lat/0402006].
23. M. G. Alford, A. Kapustin and F. Wilczek, Phys. Rev. D **59** (1999) 054502 [arXiv:hep-lat/9807039].
24. F. R. Brown *et al.*, Phys. Rev. Lett. **65** (1990) 2491.
25. P. de Forcrand and O. Philipsen, arXiv:hep-ph/0301209; Nucl. Phys. B **673** (2003) 170 [arXiv:hep-lat/0307020]; Nucl. Phys. Proc. Suppl. **129**, 521 (2004) [arXiv:hep-lat/0309109].
26. P. de Forcrand, PoS(LAT2006)130.
27. S. Ejiri, C. R. Allton, S. J. Hands, O. Kaczmarek, F. Karsch, E. Laermann and C. Schmidt, Prog. Theor. Phys. Suppl. **153**, 118 (2004) [arXiv:hep-lat/0312006].
28. R. V. Gavai and S. Gupta, Phys. Rev. D **71**, 114014 (2005) [arXiv:hep-lat/0412035].
29. S. Ejiri, T. Hatsuda, N. Ishii, Y. Maezawa, N. Ukita, S. Aoki and K. Kanaya, PoS(LAT2006)132 [arXiv:hep-lat/0609075].
30. M. A. Stephanov, Phys. Rev. D **73**, 094508 (2006) [arXiv:hep-lat/0603014].
31. M. A. Stephanov, K. Rajagopal and E. V. Shuryak, Phys. Rev. Lett. **81** (1998) 4816 [arXiv:hep-ph/9806219]; Phys. Rev. D **60** (1999) 114028 [arXiv:hep-ph/9903292].
32. P. Braun-Munzinger, K. Redlich and J. Stachel, arXiv:nucl-th/0304013.